Highly selective and label-free Love-mode surface acoustic wave biosensor for carcinoembryonic antigen detection using a self-assembled monolayer bioreceptor

P J Jandas[1], Jingting Luo[1,2]*, Aojie Quan[1], Chuanghua Qiu[3], Weiguo Cao[4], Chen Fu[1]*, Yong Qing Fu[5]

[1] Key Laboratory of Optoelectronic Devices and Systems of Ministry of Education and Guangdong Province, College of Physics and Optoelectronic Engineering, Shenzhen University, 518060, Shenzhen, PR China

[2] State Key Laboratory of Powder Metallurgy, Central South University, Changsha, PR China

[3]The First Affiliated Hospital of Shenzhen University, Shenzhen Second People's Hospital, 518035, Shenzhen, PR China

[4]Department of Radiology, Shenzhen Children's Hospital, 518038, Shenzhen, PR China

[5]Faculty of Engineering and Environment, Northumbria University, Newcastle upon Tyne, NE1 8ST, UK

Prof. Jingting Luo

Key Laboratory of Optoelectronic Devices and Systems of Ministry of Education and Guangdong Province

College of Physics and Optoelectronic Engineering

Shenzhen University, 518060, Shenzhen

PR China

Email: luojt@szu.edu.cn chenfu@szu.edu.cn

Abstract

A love-mode surface acoustic wave (SAW) biosensor based on ST-cut quartz was developed for highly selective and label-free detection of carcinoembryonic antigen (CEA). The delay line area of an interdigital transducer (IDT) based SAW device was coated with gold and then chemically modified through thioglycolic acid–EDC/NHS reaction mechanism. A self-assembled monolayer of anti-CEA was further immobilized on the bioreceptors through the coupling layer. The biosensing capability of the SAW device was evaluated using solutions of CEA with various concentrations and limit of detection was obtained at 0.31 ng/ml of CEA, which is better than the results reported by the literatures available for CEA detection using SAW device. The real-time detection capability of the biosensor was evaluated using clinical serum samples and selectivity was evaluated using mixed solutions of CEA with other common tumor marking proteins. Long-term stability of the biosensor was also evaluated over a period of 30 days and the biosensing performance has shown only 8% decrease in performance within the whole period. The binding of CEA onto the bioreceptor was evaluated through Langmuir and Freundlich sorption isotherm kinetic studies as well.

Keywords: *SAW; CEA; SAM; Piezoelectricity; Label free; Biosensing.*

1. Introduction

Piezoelectric sensors have been established as one of the key sensing technologies for a wide range of applications [1] including gas sensing [2], humidity and environmental studies [3], tumour diagnosis [4], food analysis [5], blood and other body fluids examination [6]. Among these piezoelectric sensors, surface acoustic wave (SAW) and quartz crystal microbalance (QCM) sensors are two important and popular analytical tools. SAW-based sensors have advantages such as real-time and label-free detection capabilities, wireless and remote control functions and simplicity in operation. The popularity of the SAW device is also attributed to its high sensitivity, small size, affordable cost and easy data analysis [7]. SAW based humidity sensors for environmental monitoring are largely popular today [8, 9]. Fertier et al. have reported the biosensing capability of SAW device towards various peptides through a novel semicarbazide transducer bioreceptor surface based on self-assembled monolayer (SAM) [10]. Love and Rayleigh modes of SAW devices were also utilized as effective methods for methane sensing by Wang et al. [11]. Zhang et al. applied SAW device for marine toxicity evaluation [12]. Sayago et al. developed a Love wave sensor for the recognition of chemical warfare agent stimulants [13].

The essential part of the SAW instrument consists of a piezoelectric device prepared either from quartz, lithium niobate or lithium tantalite, or any other piezoelectric materials and thin films [1]. Variation in the piezoelectric output (e.g., frequencies and phase angles) of the delay line based device indicates the extent of changes happened on the delay line area (typically the middle part of the SAW device). To obtain the output signals, two metal interdigital transducer (IDT) electrodes are prepared on both sides of the SAW device, one as emitter and another as a receptor for SAW. The waves generated from the emitter propagate through the delay line area to reach the receptor part, where it is further converted

into the corresponding electrical pulse. Any changes on the delay line area as a result of chemical/biological reactions will be reflected by the output electrical pulse since such perturbations can change the propagation velocities of the SAW [14]. During biosensing process, adsorption of biomolecules on the delay line area may result in a mass increase on the device surface, ultimately altering the centre frequency of the SAW device. The intensity of the change considers as corresponds to the extent of mass deposition on the delay line area and can be determined by a suitable oscillator circuit [15]. Therefore, a suitably prepared bioreceptor on the delay line area of SAW device can be used as a selective and sensitive layer for sensing of various biomolecules [16].

SAW devices are now becoming popular for the detection of tumour marking proteins. For example, it can be used for early identification of cancer, which is based on the detection and estimation of tumour marking protein in body fluids [17]. Conventional methods such as radioimmunoassay (RIA), enzyme-linked immunosorbent assay (ELISA) and fluoroimmunoassay (FIA) and chemiluminescence immunoassay (CLIA) are commonly used for these cancer detection purposes. However, tedious analyte sample preparative method, complicated analysis process, relatively long time of analysis, use of expensive instruments and requirement of well-trained staff for performing the analysis cause the pressure to find better detection methods or alternatives for these types of applications [18].

Carcinoembryonic antigen (CEA) is a tumour marking protein, which presents in high concentration (>20ng/ml) in human body affected by colorectal, lung, liver, ovarian, stomach, pancreatic or breast cancers [19]. Presence and various stages of cancer can be identified through the estimation and analysis of CEA in the body fluids. A real-time, highly sensitive and selective biosensor can make the diagnosis of such disease conditions much easier. For example, Huang et al. reported a disposable electrochemical SAW sensor for the

detection of CEA from clinical serum samples [20]. Chen and Tang, on the other hand, reported about QCM based CEA biosensor with a detection limit of 0.5ng/ml [21]. Zhang et al. used SAW biosensor to detect CEA from exhaled breath condensate and achieved a limit of detection 1ng/ml. They prepared anti-CEA based SAM layer on the SAW device to attract CEA molecules through non-covalent based sorption process. Alizadeh et al. developed a paper-based microfluidic colorimetric immunosensor for CEA estimation with a limit of detection of 0.51pg/ml [22].

In the present study, a SAW-based biosensor was developed for the real-time label-free detection of CEA using a novel preparation method of anti-CEA SAM bioreceptor. Immobilization of antibody on the SAW delay line for the liquid state analysis conditions always remains a major challenge for the biosensor preparation and many of the existing methods are either not suitable for biomolecular immobilization on the SAW device or cause high insertion loss. In the present study, a covalent bridging of anti-CEA has been established for a sensitive, selective and stable biosensing performance through Au coating of SAW delay line and attaching bridging units through thioglycolic acid – ethyl-dimethyl-aminopropyl carbodiimide (EDC)/ N-Hydroxy Succinimide (NHS) reaction method. This bridging unit can be further successfully used to host the antibody molecules through the reaction between its activated acidic end and amine moieties of anti-CEA. Initially, a SAW device was made on ST-cut quartz substrate with a delay structure and the delay line area was then coated with Au thin layer and a SAM of anti-CEA was immobilized as mentioned above. For the biosensing study, a microfluidic chamber was fabricated and CEA solutions with various concentrations were analysed using a SAW sensor and the limit of detection was estimated. The real-time detection capability of the biosensor was evaluated by analysing clinical serum samples. Selectivity and long term stability of the biosensor were

further determined. The ease of sorption of CEA on the bioreceptor was theoretically evaluated using Langmuir and Freundlich isotherm kinetics.

2. Experimental

2.1. Materials

CEA, anti-CEA, alpha-1-fetoprotein (AFP), cancer antigen 125 (CA125) and L-tryptophan, bovine serum albumin (BSA, 96-99%), thioglycolic acid, EDC, NHS and other common chemicals were purchased from Sigma Aldrich, USA. Clinical serum samples were supplied by the Second People's Hospital, Shenzhen, China. Removable chemical protective coating used for the IDTs, Protectapeel, was purchased from Spaylat International, UK. The phosphate buffer solution (PBS) was prepared using K_2HPO_4 and $KHPO_4$ and pH value was adjusted to be 7.4. Bovine serum albumin (BSA, 10 mg/ml) was used to block the unrecognized adsorptions. CEA solutions with different concentrations of 0.1, 1, 5, 10, 20 and 30 ng/ml were prepared in PBS solution and stored in sterile conditions. All the testing solutions were freshly prepared before each usage.

3. Method

3.1. SAW biosensor device preparation

Single side polished ST-cut quartz wafer (4 inch in diameter) was used to fabricate SAW devices for biosensor. Two IDTs were prepared on SAW device using Au electrode with 150 nm thickness and 60 finger pairs. The delay line area was at the exact middle of input and output IDTs (4mm from each side). The quartz substrate was cleaned using acetone, isopropyl alcohol, and deionised (DI) water, followed by drying under nitrogen flow. A negative UV photoresist (SU--8) was spin coated onto quartz substrate and thickness of photoresist was maintained at about 2μm, under a spin coating speed of 2500rpm for 60 seconds. The coated wafer was baked at 90°C for 90 minutes and then exposed to UV light

source for 2 seconds. The substrate was baked again for 30 seconds at 95°C and 80s at 102°C. In the next stage, the substrate was immersed in the developer solution for 40 seconds. Finally, the photoresist was removed by immersing the substrate in acetone.

Au coating of ~100nm thickness was adopted to fabricate the transducers of the SAW delay line using electron beam physical evaporation method. In addition, a gold film for SAM purpose on the delay line area was deposited using a magnetron sputtering source with a gold target (3.8 cm diameter). The argon sputter gas pressure during the deposition was maintained at 1.5×10^{-3} mbar. The target-to-substrate distance was kept at 19 cm and the substrate was rotated at 3.6 rpm. The power and the deposition time were maintained at 100 W and 30 mins, respectively.

SAM based bioreceptor preparation on the Au coated device

The SAW device was cleaned using acetone and the areas other than delay line (Au coated) were protected using chemical protective coating Protectapeel. Afterwards, the Au delay line was treated with piranha solution (1:3 H_2O_2: H_2SO_4) for 5 min. The DI water and ethanol cleaning were conducted and followed by drying under nitrogen flow. The same cleaning protocol was repeated after each chemical treatment. Thioglycolic acid treatment was conducted in the next stage by incubating the SAW device within the reagent (5 mM) for 12 hours. Afterwards, the surface was treated with 2 mL solution mixture of 400 mM EDC and 100 mM NHS (1:1 in volume ratio) in methanol for 3 hours. Immediately after cleaning and drying, the surface was treated with 100 g/mL of anti-CEA and incubated at 4°C and 50 ± 5% relative humidity for 12 hours. The delay line area of the SAW device was then cleaned with PBS solution and dried under nitrogen flow. Finally, the Protectapeel was carefully removed and the device was stored at 4°C and 50 ± 5% under sterile conditions to avoid any contaminations. The morphology was studied to confirm the successful formation

of the bioreceptor using a scanning electron microscope (SEM, Zeiss EVO-MA), atomic force microscope (Bruker NanoWizard®4 BioScience), optical microscope (Ningbo Sunny Technology Co. Ltd, CX40 Biological optical microscope) and contact angle measurement system (United Test Co., Ltd, CAG100 Contact Angle Goniometer).

Micro-fluidic chamber and measurement setup

The bio-sensing system integrated with a micro-fluidic chamber is illustrated in figure 1, which is connected to a single channel injecting system to provide a controlled flow of sample solution. The SAW device is electrically connected into a VNA. A specific program was developed based on Labview to record the S21 response of our delay line device in real time, and then the corresponding frequency is extract with respect to a defined phase value and saved in the PC simultaneously. Therefore, any perturbation on the delay line area affects the SAW propagation and results in a shift of the total response of S21, finally display on the plot of the tracking frequency, as is shown in Figure 2.

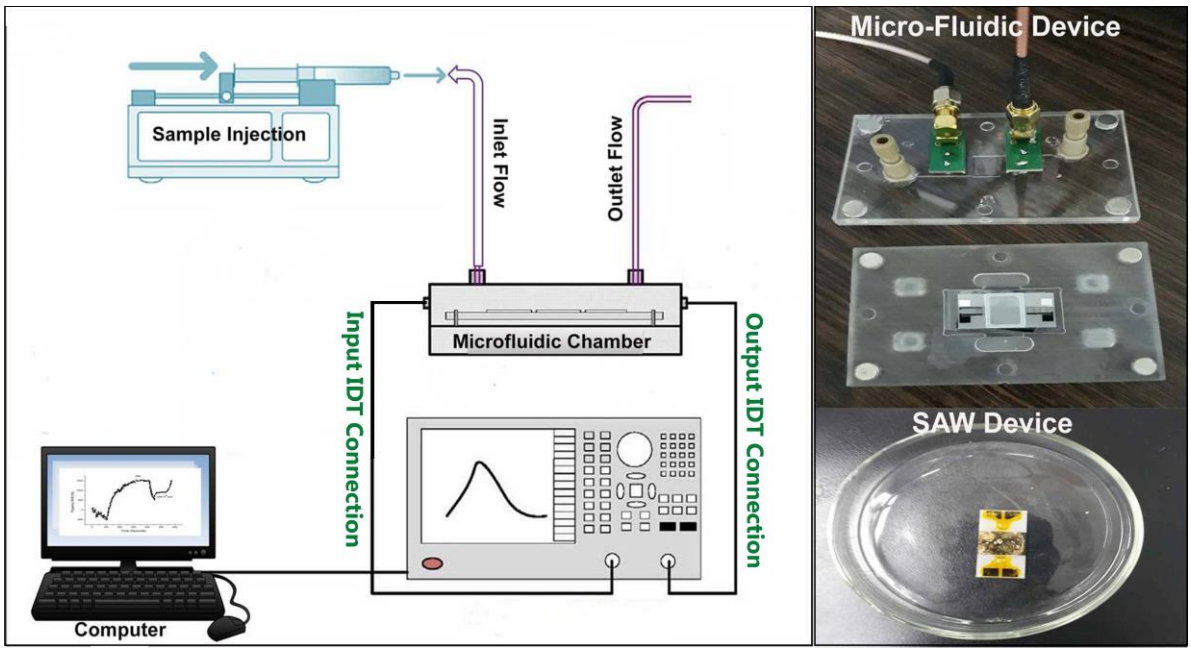

Figure 1: Biosensing set-up, microfluidic device and SAW device (SAM prepared and IDTs are protected with chemical protector)

Immunoassay analysis

Immunoassay analysis to evaluate the biosensing performance of the biosensors was conducted using CEA solutions with various concentrations from 0.1 ng/ml to 30 ng/ml. The central frequency shift of the SAW device as a function of response time at an interval of 1 seconds during each immunoassay run was recorded using a network analyser, Keysight Technologies, E5071C. The flow rate of the sample for all the immunoassay run was optimized at 0.05 ml/minute and each test was continued until an equilibrium plateau was obtained. At the end of each immunoassay run the biosensor was washed with PBS. Newly prepared bioreceptor was allowed to interact with bovine serum albumin (BSA) before exposed it to CEA samples to reduce the undesired adsorptions. A fixed volume of CEA solutions in the PBS with variable concentrations ranging from 0.1 ng/ml to 30ng/ml was allowed to flow through the receptor cell during the immunoassay analysis. Each sample was tested for 5 runs to evaluate the repeatability. The final value of frequency shift has been recorded after PBS washing at the end of each immunoassay analysis. Also, the regeneration of the bioreceptor was conducted by running a buffer solution of HCl (0.8M), KCl (0.06M) and glycine 0.06M for half an hour or until a stable plateau was obtained. Finally, the real-time analysis capability of the SAW biosensor was tested using clinical serum samples. The selectivity of the SAW biosensor was also tested using immunoassay analysis with a mixture of CEA and other common tumour marking proteins such as alpha-1-fetoprotein (AFP), cancer antigen 125 (CA125) and L-tryptophan. The results were compared with the output obtained from the corresponding solution of CEA. The stability of the SAW biosensor was tested by keeping the device for 30 days in 4°C and 50 ± 5% relative humidity and tested for immunoassay run after every 5 days of intervals.

4. Results and Discussions

4.1. SAM Bioreceptor preparation

The basic insertion loss of the SAW device in the air was -18 dB at the operating frequency of 123 MHz, and -20 dB in the PBS flow. Then it dramatically dropped into -26 dB after the bioreceptor preparation. The increase of insertion loss was regarded as the absorption of the acoustic wave due to the presence of SAM bioreceptor materials on the delay line area.Since the present investigation was concentrated on the liquid state analysis, the frequency shift of the SAW device was monitored under PBS flow before and after the preparation of the SAM bioreceptor, as is shown in Figure 2.

Considering the PBS run, successful formation of the SAM on the delay line area of the SAW device was found to reduce the frequency shift by ~310 Hz. Thioglycolic acid can form a coordination bond with the Au molecules coated on the delay line of the SAW device. This can facilitate an effective bonding with anti-CEA and thus form a uniform SAM on the SAW device [24]. The chemistry behind the SAM preparation is depicted in figure 3. The EDC/NHS treatment on the thioglycolic acid on the Au surface in the next step tends to form a sterically unstable intermediate complex. This reactive ortho-acylisourea can further form amide linkage with the amine groups of anti-CEA through substitution reaction, which ultimately allows the immobilization of anti-CEA on the device surface as a SAM layer.

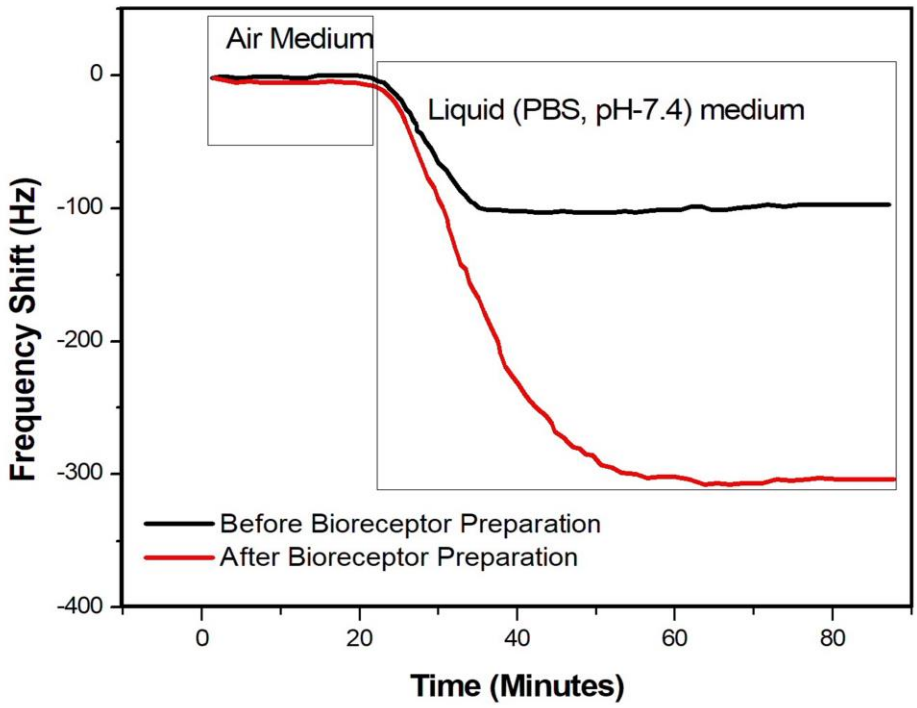

Figure 2: Frequency shift of S21 response under air and liquid run (PBS) before and after the preparation of bioreceptor

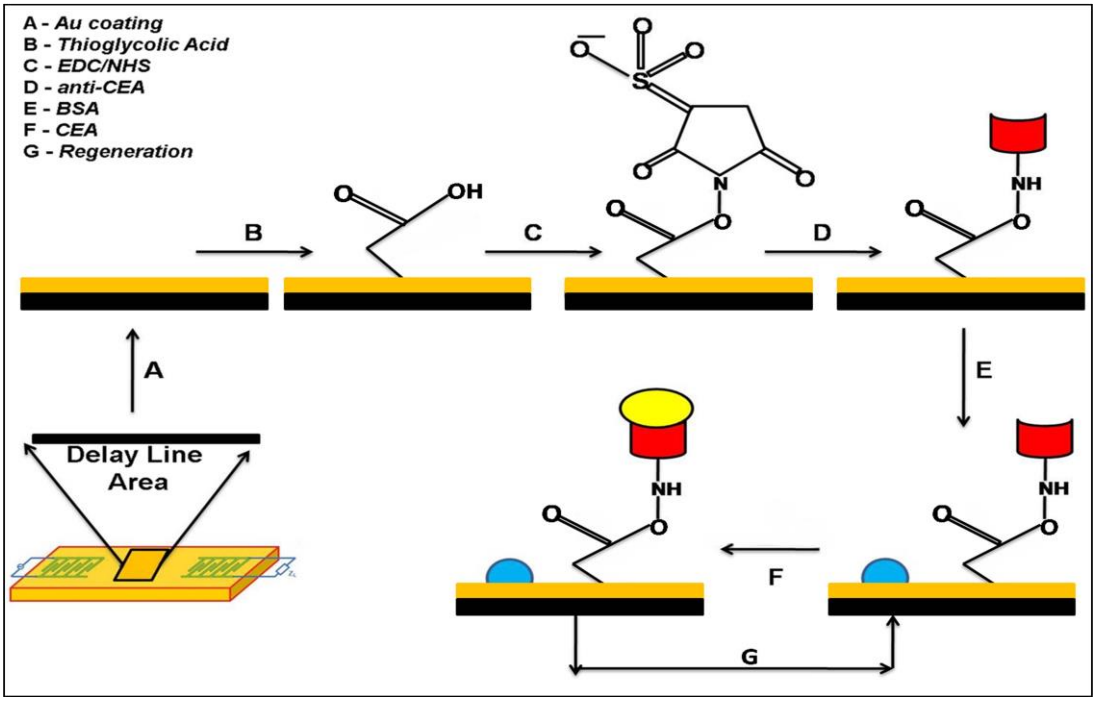

Figure 3: Scheme of bio-sensing in the present study

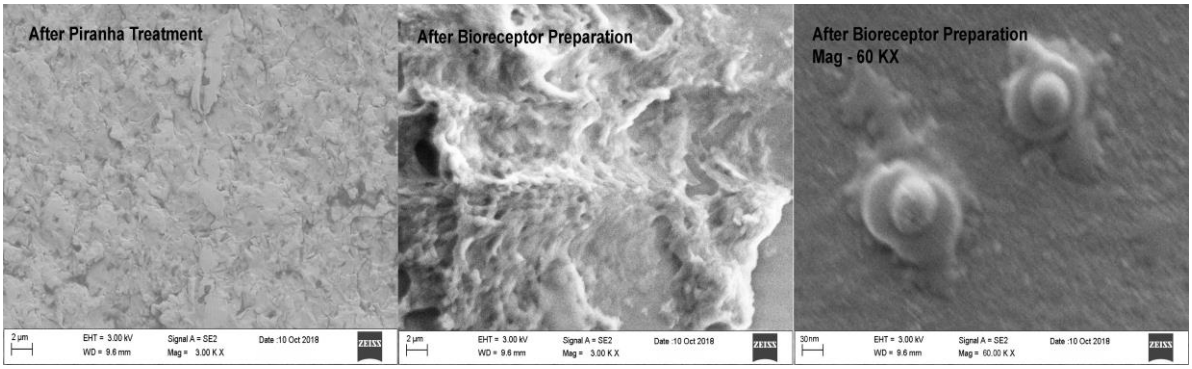

Figure 4: SEM mages of delay line area after chemical degreasing and SAM preparation

The morphological analysis using AFM, SEM and optical microscopy were used to confirm the successful formation of bioreceptor on the SAW device. Figure 4 represents the SEM of the original and SAM prepared Au delay line of SAW devices. The rough morphology of untreated surface is due to the degreasing process using piranha solution. The rough morphology can provide more surface area to interact with the thioglycolic acid molecules, which then forms the SAM layer. Whereas, the SAM formation on the SAW device has changed the morphology and the thin film of SAM is visible in the micrograph. The magnified SEM image is given in the Figure 4, in which the reaction nuclei are clearly visible, which is due to the larger size of anti-CEA molecules.

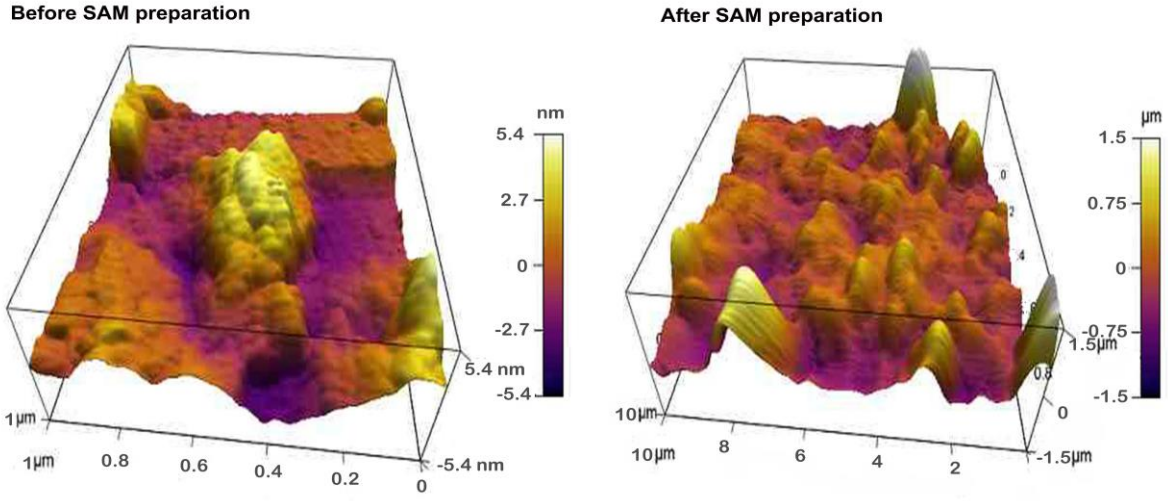

Figure 5: AFM images of delay line surface before and after the bioreceptor preparation

Figure 4 shows the AFM images of original and SAM prepared Au surface of SAW device as well. According to the figure, the added thin film on the SAW device has changed the AFM dimensions of untreated surface considerably. The ups and troughs on the AFM image on the SAW device are clearly increased in sizes after the SAM formation as compared to the untreated surface. This indicates the successful immobilization anti-CEA molecules on the surface of the SAW device. Change in morphology by the successful formation of SAM on the Au coated delay line of SAW device was confirmed using optical microscopy as well. The micrograph of the untreated surface was unable to record due to the high level of reflection of the Au surface. However, the formation of SAM on the Au surface allows the recording the fluorescent image. Figure 6, represents the obtained optical micrograph of the SAM coated SAW surface. The small darker spots on the micrograph may be the reaction nuclei present on the SAM layer.

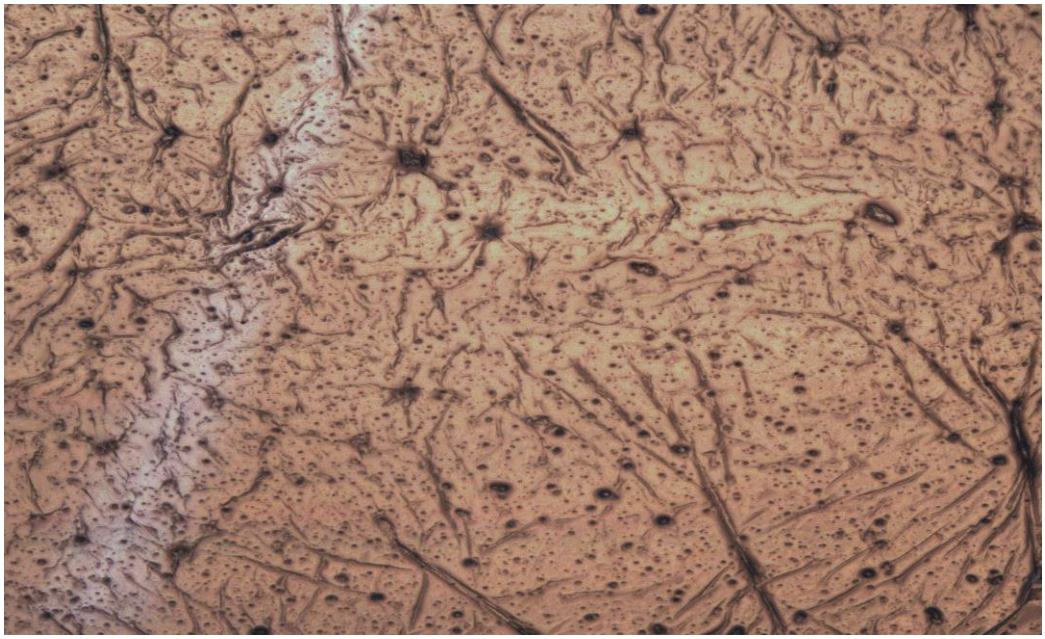

Figure 6: Fluorescent microscopic image of SAM

Figure 7: Contact angle of the delay line surface before and after the SAM preparation

Hydrophilic nature of the bioreceptor surface is critical to influence the biosensing property. Since the biomolecules are highly hydrophilic in nature, the bioreceptor surface also needs to be hydrophilic in order to facilitate easy interaction with the anlyte biomolecules. Formation of SAM can provide polar entities on the bioreceptor surface which can enhance the hydrophilicity of the SAW surface. This has been confirmed using contact angle studies and the results are shown in Figure 7. The untreated SAW surface has a contact angle of 80°, but this was reduced to 20.5° after the formation of SAM, which has further confirmed the successful formation of SAM.

4.2. Immunoassay response of Au coated SAW biosensor

The immunoassay analysis has been conducted using the multi-stage device and the setup is shown in Figure 1. Sample injection system consists of a flow regulator, which is connected with the biosensor setup. Various CEA solution samples with concentrations ranging from 0.1ng/ml to 30 ng/ml were generated using a 5 ml syringe and allowed to pass through the SAW biosensor placed within the microfluidic chamber. The successful sorption of CEA on the anti-CEA based SAM can cause a mass load on the delay line area of the SAW device and thus changes the response of S21 parameter. The resulting frequency shift with respect

to the CEA capture was recorded via the program automatically during each immunoassay analysis.

One example recorded in the immunoassay analysis of the present study is given in figure 8a. The average values of frequency shift for each CEA concentrations are given in Figure 8b (standard deviations are shown as error bars) and the calibration curve in log-log plots as Figure 8c. The concentration of 0.1 ng/ml did not result in any considerable change in the base frequency, so the corresponding frequency response is not given in the figure. The frequency shift of the SAW device was found to decrease linearly with the increase in the concentration of the CEA solutions. This suggests a favourable shift in equilibrium towards the forward reaction, adsorption of CEA on anti-CEA, with the increase in concentration. According to figure 8b, the increase in the concentration of CEA solution tends to enhance the difference in frequency shift between the sample run and base frequency. The consistency in the results found good since standard deviation values reported lay within 4-8% of the average values reported for each concentrations. The response time of the bioreceptor also found faster as the equilibrium plateau attained within a time period of 30-40 minutes for all immunoassay run. The limit of detection of the biosensors was calculated as blank frequency response by PBS + 3 × Noise (standard deviation) according to et al. [32]. The detection limit was calculated as 0.31 ng/ml of CEA concentration. Comparative data about the limit of detection obtained by various studies from literature survey are summarized in Table 1. The upper limit of the biosensor was evaluated experimentally and the results are given in the supportive data, Figure S1. Till 80 ng/ml the bioreceptor responded with a steady increase in variation in frequency shift. However, above this concentration level the biosensor showed saturation nature. The efficiency of the present biosensor was also evaluated by comparing the concentration of the CEA solutions

calculated using experimental and theoretical data. Theoretical values obtained from the total flow of the known concentrations of CEA solutions for a fixed time period. Calculation of experimentally deposited mass on the SAW device during immunoassay analysis was done according to the relationship suggested by Sayago et al. [31]. The measured data of the biosensor show good agreements with the theoretical values and the results are listed in table 2.

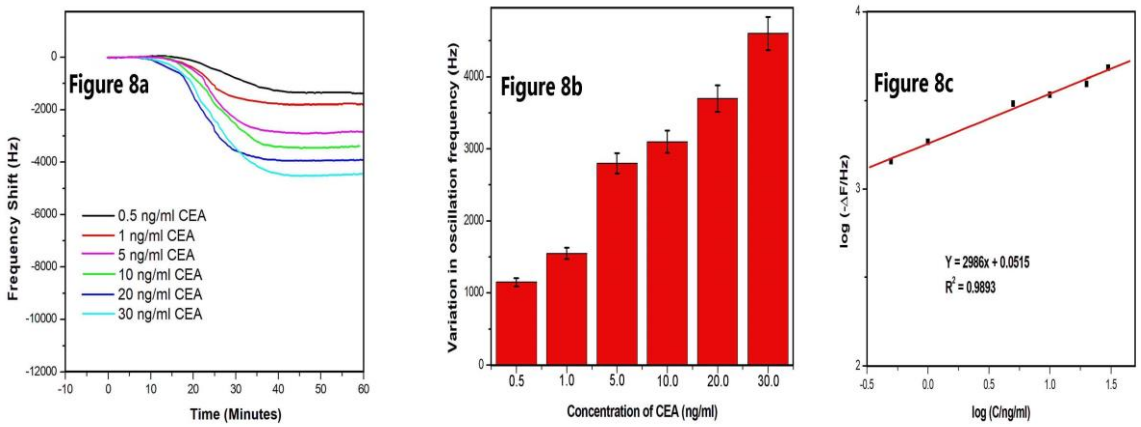

Figure 8: Immunoassay response of biosensor against CEA stock solutions

Table 1: Limit of detection reported by various studies for piezoelectric detection of CEA

Study	**Sensitivity**	**Method**
S. Li et al. [23]	37 pg/ml	Love wave –Surface acoustic wave biosensor
Chen et al. [21]	5 ng/ml	Quartz Crystal Microbalance biosensor
D. Zheng et al. [25]	0.2 mg/mL	Bulk Acoustic resonator
X. Zhang et al. [26]	1 ng/ml	Surface acoustic wave biosensor
Present Work	0.31 ng/ml	Surface acoustic wave

	biosensor

Table 2: Comparative results of the actual and experimental estimation of mass deposition of CEA in each immunoassay run.

The concentration of CEA stock solution (ng/ml)	**0.5**	**1**	**5**	**10**	**20**	**30**
Experimental value (ng)	1.2±0.4	2.4±0.6	12.9±2.6	26.7±5.9	53.8±8.7	79.7±7.3
Theoretically calculated value (ng)	1.5	3	15	30	60	90

The sorption equilibrium was studied to understand the favourability of antigen –antibody interaction using Langmuir and Freundlich sorption kinetics [27, 28]. According to Langmuir sorption isotherm,

$C_e/q_e = (1/q_0 b) + (C_e/q_0)$

where C_e is the equilibrium concentration (mg/L) of CEA stock solutions, qe is the equilibrium sorption capacity (mg mg^{-1});, the constant q_0 indicates the real sorption capacity (mg mg−1) of the biosensor and b is related to the energy of sorption (L $mmol^{-1}$). The constant values have been adopted from the previously published works [27,28] and the isotherm curves is plotted as C_e/q_e v/s C_e, as shown in figure 9. The date points can be fit into a straight line which indicates that the sorption process during the immunoassay experiment in the present study follows Langmuir kinetics. The slop and intercepts were calculated as 2.25 mmol/g and 2.71 L $mmol^{-1}$ respectively. The values represent the sorption capacity and the energy of sorption of the biosensor respectively. Also the isotherm enables to calculate the kinetic constants of adsorption (k_a) and desorption (k_d) as 2983 ±

482 L mol^{-1} s^{-1} and 5.93 ± 1.94) × 10^{-4} s^{-1} [33]. A non-zero dissociation constant value suggests existing equilibrium within the A-CEA – CEA interface. Additionally $\Delta G_{sorption}$ is calculated as well at -5.7 ±0.78 kcal mol^{-1} which is a comparable value with the previous analysis reported a favourable adsorption process [34].

The additional evidence for the favourable sorption process during the immunoassay run can be extracted through the modified form of Langmuir relation, Freundlich sorption kinetics as follows [29];,

$ln\ q_e = \ln K_f + (1/n)\ ln\ C_e$

where K_f and n are Freundlich sorption isotherm constants, which provide the information about the sorption capacity and intensity of sorption in the present case of the biosensor. The values can be calculated from the intercept and slope of the plot of ln q_e v/s ln C_e (figure 9). K_f was found to be 0.574 and n to be 3.16. The straight line shown in the graph suggests that the kinetics follows the Freundlich sorption isotherm with a better match than that of Langmuir kinetics. The further proof of the favourability for the adsorption process of CEA on the present SAM can be obtained by calculating the dimensionless constant separation factor "R_L," [30]. The value can calculate as below,

$R_L = 1/(1 + xC_0)$

where "x" is the term represent the energy or the intensity of the sorption process. According to the concept, the parameter R_L depends on the shape of the isotherms and favourability of sorption can be evaluated as below,

RL > 1, unfavourable

RL = 1, linear

0 < RL < 1, favourable

RL = 0, irreversible.

In the present study, the isotherms have suggested favourable values for R_L, since both the relations suggested values <1 and <0. Moreover, Freundlich sorption isotherm has given a better fit with a value of 0.891 as compared to the Langmuir value 0.855.

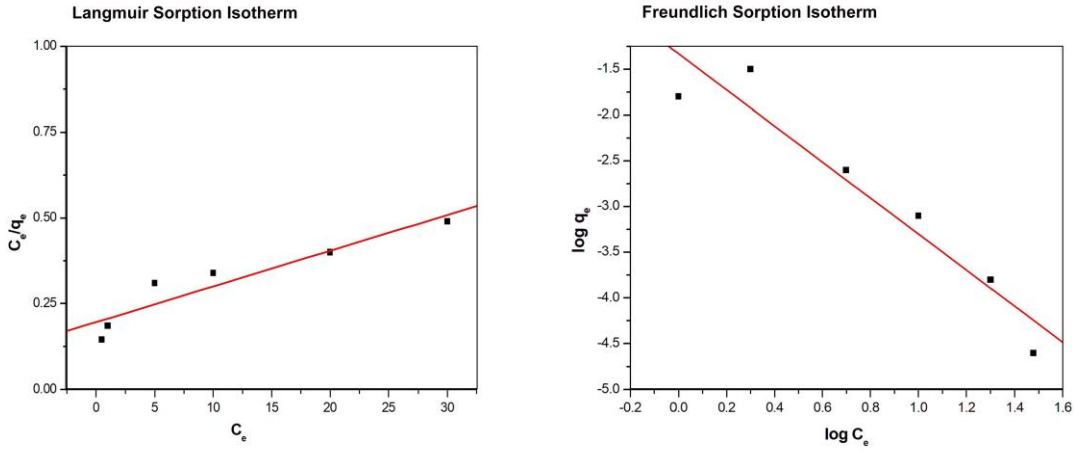

Figure 9: Sorption kinetic using Langmuir and Freundlich isotherms

4.3. Analysis of clinical serum samples

The real-time applicability of the newly developed biosensor was conducted using clinical serum samples. The sample analysis was conducted in collaboration with Second People's hospital, Shenzhen China. According to the hospital records, the sample collection was conducted as a part of their initial diagnosis before confirming the disease in patients who were suspected to have colorectal cancer. Twelve of serum samples were collected and analysed using our SAW biosensor and the results were compared with the ELISA results, which are listed in table 4. The samples for analysis were prepared by adding 0.5mL serum in 2mL of PBS solution with a pH value of 7.4. According to the biosensor results, only 3 of the samples were suspected to be from colorectal cancer affected patients. Sample number 3, 8 and 12 have given the CEA concentration 21, 27 and 26 ng/ml, which were suggested for further confirmation analysis. The remaining samples contained less than 5 ng/ml of CEA. The results were in good agreements with those obtained from the ELISA analysis.

However, the present biosensor has shown much better consistency of the results, which produces a smaller standard deviation and also a faster analysis time (30-50 minutes), and is much better than that of ELISA method (6-8 hours).

Table 4: Validation of the biosensor using clinical serum sample analysis

Sample No.	SAW Biosensor results (ng/ml)	ELISA (ng/ml)
1	0.59±0.24	0.64 ±0.34
2	0.81±0.30	0.85 ±0.4
3	21.96±3.16	21.28 ±4.5
4	1.35±0.12	1.41 ±0.31
5	1.93±0.29	2.06 ±0.31
6	2.28±0.41	2.62 ±0.48
7	2.87±0.33	2.95 ±0.41
8	27.93±2.28	30.07 ±4.34
9	3.31±0.81	3.28 ±1.01
10	3.68±0.22	3.73 ±0.82
11	4.64±0.31	4.77 ±0.65
12	26.14±3.24	26.15 ±5.21

4.4. Selectivity of the biosensor

The selectivity of the biosensor was evaluated by conducting the immunoassay analysis with a mixture of CEA solution (0.5ng/ml) and common tumour marking proteins including alpha-1-fetoprotein (AFP), cancer antigen 125 (CA125) and L-tryptophan. The compositions of the tested samples are listed in Table 5. Figure 10 shows the representative

image of immunoassay responses. According to the results, the biosensor did not show any considerable affinity towards the other tumor marking proteins, except the CEA. The equilibrium frequency shift obtained for each immunoassay run was within the range obtained from the pure CEA solution. The results suggest the prepared biosensor has a good selectivity towards CEA tumor marking proteins and it has a negligible affinity on the other tumor proteins.

Table 5: Combination of tumor markers used for each selectivity test

Tumor Marker	**CEA (ng/ml)**	**AFP(ng/ml)**	**CA125(ng/ml)**	**L-tryptophan (ng/ml)**
a	0.5	0.5	0	0
b	0.5	0	0.5	0
c	0.5	0	0	0.5

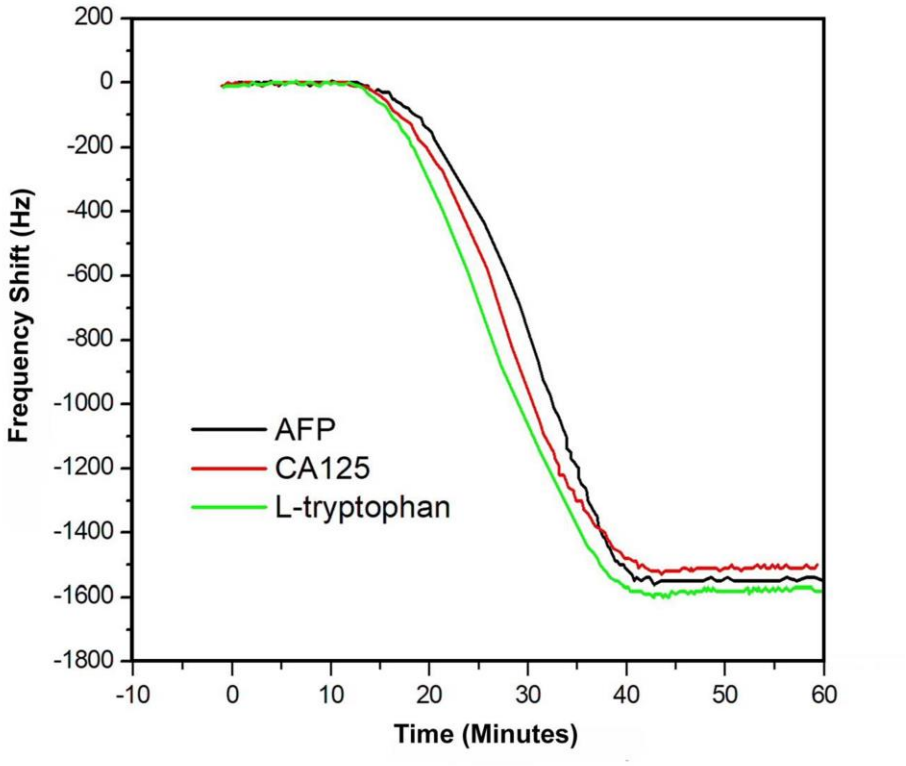

Figure 10: Immunoassay response against a mixture of tumour marking proteins

4.5. Long term stability of the Biosensor

The biosensor was further tested for its consistency of sensing result for a period of 30 days. A batch of 10 biosensors was used for this purpose and the average values of the results were obtained and then compared with the initial results to understand the variation in biosensing performance. The immunoassay experiments were conducted for every 5 days of intervals. The performance variation in percentage with respect to the initial day results are depicted in figure 11. According to the results, the biosensor performs well within the tested time period and within 20 days of the time period the performance was decreased by only around 5% and around 8% decrease in performance was observed during the whole testing time period.

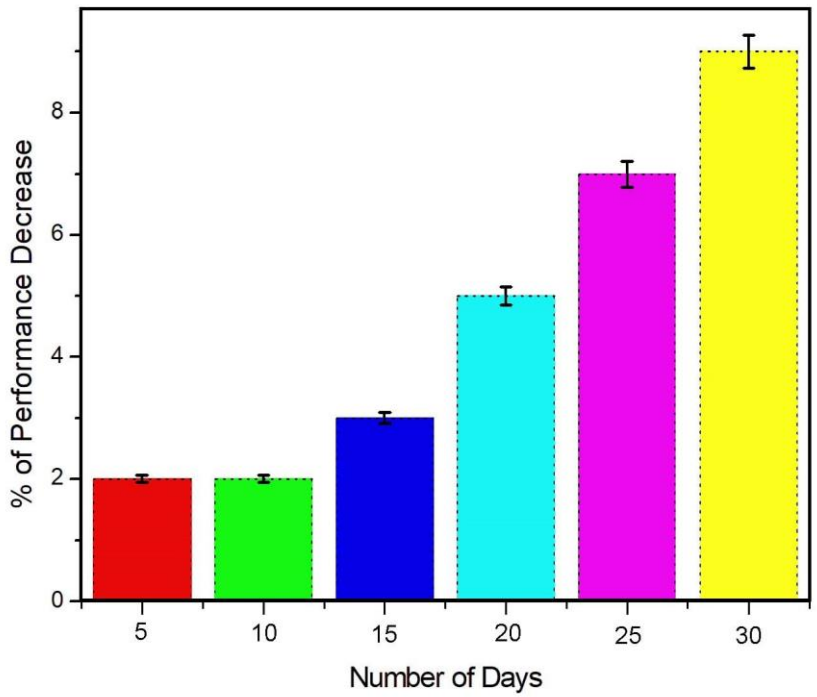

Figure 11: Long term immunoassay response of the biosensor

5. Conclusion

A SAW based biosensor for the selective detection of CEA was prepared and validated using real-time analysis of clinical serum samples. The SAW device was then modified for biomolecular immobilization through a novel method for bioreceptor preparation on SAW device for CEA detection. A controlled coating of Au thin film on the delay line area of SAW was prepared. Furthermore, the thioglycolic acid – EDC/NHS covalent interaction based immobilization method was applied to prepare a SAM of anti-CEA on the delay line. The CEA solutions with concentration from 0.1 to 30 ng.ml were used for immunoassay analysis and a practical limit of detection of the biosensor was found to be 0.31 ng/ml. The affinity of CEA on the anti-CEA based SAM was studied through Langmuir and Freundlich sorption isotherm kinetics. The adsorption of CEA during the immunoassay process was found favourable, which follows both the isotherm concepts. The real-time detection of

clinical serum samples was conducted to validate the practical applicability of the biosensor. The results were in good agreements with the ELISA results and the biosensor was recorded to have a better consistency and a fast response time. The biosensor found highly selective and had no considerable deviation in the immunoassay response when tested with CEA samples in combination with other tumour marking proteins. The long term stability of the biosensor also tested and within a time period of 30 days of usage the average performance was found to decrease around 8%.

Acknowledgement

The authors gratefully acknowledge the support of Research and Development Program of China (Grant no. 2016YFB0402705), National Natural Science Foundation of China (NSFC Grant no. 11704261, 11575118), Shenzhen Science & Technology Project (Grant no. JCYJ20170817100658231, JCYJ2018050718243957，JCYJ20180305124317872), Natural Science Foundation of SZU (Grant no. 2017067), Shenzhen Key Lab Fund (ZDSYS20170228105421966), UK Engineering and Physical Sciences Research Council (EPSRC) EP/P018998/1, Newton Mobility Grant (IE161019) from the UK Royal Society and the National Natural Science Foundation of China, and Royal Academy of Engineering UK-Research Exchange with China and India.

Conflict of interest

The authors do not have any conflict of interest regarding this publication.

References

[1] Petr Skladal, Piezoelectric biosensors, Trends in Analytical Chemistry, 79 (2016) 127-133

[2] Wen Wanga, Xueli Liua, Shengchao Mei, Yana Jia, Mengwei Liu, Xufeng Xue, Dachi Yang, Development of a Pd/Cu nanowires coated SAW hydrogen gas sensor with fast response and recovery, Sensors and Actuators: B. Chemical 287 (2019) 157–164

[3] Evgeni Eltzova,b, Adiel Yehudaa, Robert S. Marks, Creation of a new portable biosensor for water toxicity determination, Sensors and Actuators B 221 (2015) 1044–1054

[4] Victor Crivianu-Gaita, Mohamed Aamer Roy T. Posaratnanathan, Alexander Romaschin, Michael Thompson, Acoustic wave biosensor for the detection of the breast and prostate cancer metastasis biomarker protein PTHrP, Biosensors and Bioelectronics, 78, 15 2016, 92-99

[5] Antonis Kordas, George Papadakis, Dimitra Milioni, Jerome Champ, Stephanie Descroix, Electra Gizeli, Rapid Salmonella detection using an acoustic wave device combined with the RCA isothermal DNA amplification method, Sensing and Bio-Sensing Research 11 (2016) 121–127

[6] X. Liu, J.Y. Wang, X.B. Mao, et al., Single-shot analytical assay based on grapheneoxide-modified surface acoustic wave biosensor for detection of single-nucleotide polymorphisms, Anal. Chem. 87 (2015) 9352–9359.

[7] Zhangliang Xu, Yong J. Yuan, Implementation of guiding layers of surface acoustic wave devices: A review, Biosensors and Bioelectronics 99 (2018) 500–512

[8] R. Rimeika, D.˘Ciplys, V. Poderys, R. Rotomskis, M.S. Shur, Fast-response and low-loss surface acoustic wave humidity sensor based on bovine serum albumin-gold nanoclusters film, Sensors and Actuators B 239 (2017) 352–357.

[9] Xianhao Le, Xiaoyi Wang, Jintao Pang, Yingjun Liu, Bo Fang, Zhen Xu, Chao Gao, Yang Xu, Jin Xie, A high performance humidity sensor based on surface acoustic wave and graphene oxide on AlN/Si layered structure, Sensors and Actuators B 255 (2018) 2454–2461

[10] Laurent Fertier, Marc Cretin, Marc Rollanda, Jean-Olivier Durand, Laurence Raehm, Rémi Desmet, Oleg Melnyk, Céline Zimmermann, Corinne Déjous, Dominique Rebière, Love wave immunosensor for antibody recognition using an innovative semicarbazide surface functionalization, Sensors and Actuators B 140 (2009) 616–622

[11] Wang W., Hu H.L., He S.T., Pan Y., Zhang C.H., Dong C. Development of a room temperature SAW methane gas sensor incorporating a supramolecular cryptophane. A coating. Sensors. 2016;16:73.

[12] Xi Zhang, Jiaru Fang, Ling Zou, Yingchang Zou, Lang Lang, Fan Gao, Ning Hu, PingWang, A novel sensitive cell-based Love Wave biosensor for marine toxin detection, Biosensors and Bioelectronics, Volume 77, 15 March 2016, Pages 573-579

[13] Isabel Sayago, Daniel Matatagui, María Jesús Fernández, José Luis Fontecha, Izabel Jurewicz, Rosa Garrig, Edgar Muñoz, Graphene oxide as sensitive layer in Love-wave surface acoustic wave sensors for the detection of chemical warfare agent stimulants, Talanta, 148, 1 February 2016, Pages 393-400

[14] R. Weigel, D.P. Morgan, J.M. Owens, A. Ballato, K.M. Lakin, K. Hashimoto, C.C.W. Ruppel, Microwave acoustic materials, devices, and applications, IEEE Transactions on Microwave Theory and Techniques, 50 (2002) 738–749.

[15] Jay W. Grate, R. Andrew McGill, Dewetting effects on polymer-coated surface acoustic wave vapor sensors, Analytical Chemistry 67 (1995) 4015–4019.

[16] Jingting Luo, Pingxiang Luo, Ke Du, Bixia Zhao, Feng Pan, Ping Fan, Fei Zeng, Dongping Zhang, Zhuanghao Zheng, Guangxing Liang, A new type of glucose biosensor based on surface acoustic wave resonator using Mn-doped ZnO multilayer structure, Biosensors and Bioelectronics, 49 (2013) 512-518.

[17] H.P. Chan, C. Lewis, P.S. Thomas, Exhaled breath analysis: novel approach for early detection of lung cancer, Lung Cancer 63 (2009) 164–168.

[18] P.B. Luppa, C. Müller, A. Schlichtiger, H. Schlebusch, Point-of-care testing(POCT): current techniques and future perspectives, TrAC Trends Anal. Chem.30 (2011) 887–898.

[19] Sharma, S. "Tumor markers in clinical practice: General principles and guidelines." Indian journal of medical and paediatric oncology: official journal of Indian Society of Medical & Paediatric Oncology vol. 30, 1 (2009): 1-8.

[20] Ke-Jing Huang, De-Jun Niu, Wan-Zhen Xie, Wei Wang, A disposable electrochemical immunosensor for carcinoembryonic antigen based on nano-Au/multi-walled carbon nanotubes–chitosans nanocomposite film modified glassy carbon electrode, Analytica Chimica Acta 659 (2010) 102–108

[21] Zai-Gang Chen, Dian-Yong Tang, Antigen-antibody interaction from quartz crystal microbalance immunosensors based on magnetic CoFe2O4/SiO2 composite nanoparticle-functionalized biomimetic interface, Bioprocess Biosystem Engineering, 2007, 30:243-249.

[22] Negar Alizadeh, Abdollah Salimi, Rahman Hallaj, Mimicking peroxidase activity of Co2(OH)2CO3-CeO2 nanocomposite for smartphone based detection of tumour marker using paper-based microfluidic immunodevice, Talanta 189 (2018) 100–110

[23] S. Li, Y. Wan, Y. Su, C. Fan, V.R. Bhethanabotla, Gold nanoparticle-based low limit of detection love wave biosensor for carcinoembryonic antigens, Biosensors & Bioelectronics, 95, 2017, 48-54.

[24] Thomas Bürgi, Properties of the gold–sulphur interface: from self-assembled monolayers to clusters, Nanoscale, 2015, 7, 15553–15567

[25] D. Zheng, J. Xiong, P. Guo, Y. Li, S. Wang, H. Gu, Detection of a carcinoembryonic antigen using aptamer-modified film bulk acoustic resonators, Material Research Bulletin, 59, 2014, 411-415.

[26] X. Zhang, Y. Zou, C. An, K. Ying, X. Chen, P. Wang, Sensitive detection of carcinoembryonic antigen in exhaled breath condensate using surface acoustic wave immunosensor, Sensors & Actuators B: Chemical, 217, 2015, 100-106.

[27] W.J. Weber, Physicochemical Processes for Water Quality Control, Wiley-Interscience, 1972.

[28] Farabi Temel, Egemen Ozcelik, Ayse Gul Ture, Mustafa Tabakci, Sensing abilities of functionalized calix[4]arene coated QCM sensors towards volatile organic compounds in aqueous media, Applied Surface Science 412 (2017) 238–251

[29] O. Hamdaoui, Dynamic sorption of methylene blue by cedar sawdust and crushed brick in fixed bed columns, J. Hazard. Mater. 138 (2006) 293–303.

[30] M. Rao, A.V. Parwate, A.G. Bhole, Removal of Cr6+ and Ni2+ from aqueous solution using bagasse and fly ash, Waste Manage. 22 (2002) 821–830.

[31] I. Sayago, M.J. Fernández, J.L. Fontecha, M.C. Horrillo, C. Vera, I. Obieta, I. Bustero, New sensitive layers for surface acoustic wave gas sensors based on polymer and carbon nanotube composites, Sensors and Actuators B 175 (2012) 67– 72

[32] Ronghui Wang, Lijun Wang, Zachary T. Callaway, Huaguang Lu, Tony Jun Huang, Yanbin Li, A nanowell-based QCM aptasensor for rapid and sensitive detection ofavian influenza virus, Sens Actuators B Chem, 240 (2017) 934–940

[33] D. S. Karpovich, G. J. Blanchard, Direct measurement of the adsorption kinetics of alkanethiolate self-assembled monolayers on a microcrystalline gold surface, Langmuir. 10 (1994) 3315-3322.

[34] M. Yang, M. Thompson, W. C. Duncan-Hewitt, Interfacial Properties and the Response of the Thickness-Shear-Mode Acoustic Wave Sensor in Liquids, Langmuir. 9 (1993) 802-811.